Tomographic Particle Image Velocimetry for Flow Analysis in a Single Cylinder Optical Engine

Article *in* SAE International Journal of Materials and Manufacturing · January 2015

DOI: 10.4271/2015-01-0599

CITATIONS
10

READS
311

3 authors:

Akhilendra Pratap Singh
Indian Institute of Technology Kanpur
102 PUBLICATIONS **3,619** CITATIONS
SEE PROFILE

Aditya Gupta
The University of Texas at Arlington
2 PUBLICATIONS **14** CITATIONS
SEE PROFILE

Avinash Kumar Agarwal
Indian Institute of Technology Kanpur
582 PUBLICATIONS **23,244** CITATIONS
SEE PROFILE

2015-01-0599
Published 04/14/2015

doi:10.4271/2015-01-0599
saematman.saejournals.org

Tomographic Particle Image Velocimetry for Flow Analysis in a Single Cylinder Optical Engine

Akhilendra Pratap Singh, Aditya Gupta, and Avinash Kumar Agarwal
Indian Institute of Technology

ABSTRACT

Better understanding of flow phenomena inside the combustion chamber of a diesel engine and accurate measurement of flow parameters is necessary for engine optimization i.e. enhancing power output, fuel economy improvement and emissions control. Airflow structures developed inside the engine combustion chamber significantly influence the air-fuel mixing. In this study, in-cylinder air flow characteristics of a motored, four-valve diesel engine were investigated using time-resolved high-speed Tomographic Particle Imaging Velocimetry (PIV). Single cylinder optical engine provides full optical access of combustion chamber through a transparent cylinder and flat transparent piston top. Experiments were performed in different vertical planes at different engine speeds during the intake and compression stroke under motoring condition. For visualization of air flow pattern, graphite particles were used for flow seeding. In the experiments, highly swirling air flow pattern was found, which was dominant in the vicinity of valves. Swirling patterns significantly affected by engine speed and increased at higher engine speed. The average structure of the flow field was analyzed, which showed a clear orientation of the average velocity, which changed during different phases of the cycle. Vorticity analysis showed higher vorticity beneath the intake valve that affects turbulence in air flow. Different components of velocity as Vx, Vy and Vz showed that engine speed and z-location affected all velocity components in which maximum variation takes place in Z-direction.

CITATION: Singh, A., Gupta, A., and Agarwal, A., "Tomographic Particle Image Velocimetry for Flow Analysis in a Single Cylinder Optical Engine," *SAE Int. J. Mater. Manf.* 8(2):2015, doi:10.4271/2015-01-0599.

INTRODUCTION

Airflow structures generated inside the cylinder of an internal combustion engines influence the fuel-air mixing significantly during compression stroke. Hence accurate measurement of these structures becomes very important to optimize the engine power output, fuel economy and emissions control. Several research groups carried out endoscopic optical diagnostics in IC engines however results obtained by these experiments were unable to explain air flow characteristics due to limited access [1, 2, 3]. Dierksheide et al. [1] performed PIV measurements using endoscope, CCD camera for image capturing and laser sheet for illumination.

Particle Image Velocimetry is a technique which is non-intrusive in nature and has been in practice for many years now and is being widely used for doing flow visualization of fluids. In this technique, the fluid flow is seeded with tracer particles and a laser sheet illuminates the tracer particles in the fluid flow. High speed cameras in double exposure mode are used to capture images of the seeded flow and instantaneous velocity fields are generated from the images captured using auto-correlation or cross-correlation techniques which provide data about the velocity and direction of flow in the area of interest [4, 5, 6, 7]. A lot of work has been performed for IC engine in-cylinder flow analysis more prominently in SI engines as compared to diesel engines. Basic objectives of these studies were to characterize velocity profile of air, turbulent characteristics of airflow that affects air-fuel mixing. Several researchers have performed PIV experiments for characterization of turbulence properties, spatial flow structures and influences of cycle-to cycle variations [8, 9, 10, 11, 12, 13]. Bucker et al. [5] performed stereoscopic PIV for in-cylinder flow visualization. Reuss et al. [10] studied large scale turbulent structures in directed and undirected IC engine flows and their cyclic variability. Funk et al. [9] studied turbulence properties in high and low swirl in cylinder flows. But these findings were only able to resolve 2D planar Velocity. Muler et al. [13] studied flow field in a direct injection spray guided optical engine at 500, 1000 and 2000 rpm and analyzed the cycle to cycle variation. Researchers have varied several parameters and tried to optimize the PIV systems to get good and accurate results. They studied the effects of particle image diameter, interrogation region area, seeding density, in plane and out of plane particle movement, interrogation region pixel resolution [14, 15, 16, 17, 18, 19]. Reeves et al. [20] performed 2-D flow measurements in an optical SI engine for real time flow visualizations in horizontal and vertical planes. Voisine et al. [12] investigated air flow characteristics using two component PIV and analyzed spatial structure of flow and its temporal evolution. Stansfield et al. [21] carried out in cylinder 2-D PIV measurements at different engine speeds and also calculated tumble ratios from the obtained vector fields. They used two engine speeds and found significant change in air velocity flow structures. Calendini et al. [22] was the first to perform stereoscopic PIV to resolve three components of velocity in an IC engine. Dannemann et

al. [23] performed planar PIV experiments at different crank angle positions using motored condition. They measured flow field in eight axial planes and presented 3D velocity structures.

Although stereoscopic PIV was found capable for third velocity component in an engine but spatial derivatives and three dimensional flow structures have not much studied. Hence in-cylinder measurements of the instantaneous 3D flow field are the next level for better understanding of turbulent mixing of air and fuel inside the combustion chamber. There are several techniques have been developed for 3D imaging in which 3D particle tracking velocimetry (PTV), 3D light sheet scanning PIV, holographic PIV and Tomographic PIV (TPIV) are significantly adopted by researchers [24, 25, 26, 27]. 3D PTV technique is based on low seeding densities that results sparse vector fields and holographic PIV technique works on chemical processing of the photographic holographic plates.

Elsingaet al. [28] introduced TPIV method in which Tomographic reconstruction of the 3D particle distribution was performed by volumetric correlation of the reconstructed particle distribution. Baum et al. [29] used Tomographic particle image velocimetry (TPIV) within a motored direct-injection spark-ignition (DISI) optical engine to investigate the instantaneous volumetric flow field during intake and compression stroke. Tomographic PIV is a flow visualization technique which enables us to resolve all three components of velocity in a 3D measurement volume. The volume can be varied from very thin to thick volumes. MART Algorithm (Multiplicative Algebraic Reconstruction Technique) is used to do the construction and 3D cross correlation is done to return 3D velocity data in the measurement volume. Tomographic PIV technique is very relevant in IC Engines for instantaneous flow visualization where the air flow inside the cylinder is highly varying inside in volume.

Limitation in optical access, physical space surrounding the engine, thick curved glass cylinder and engine vibration causes major problems in 3D PIV. In the present investigation, single cylinder optical engine with quartz window was used for Tomographic PIV investigation. Two different engine speeds (1200 rpm and 2100 rpm), two piston positions (270°bTDC and 90°bTDC) in intake and compression stroke and five different Z locations were investigated for velocity, vorticity and different component of velocity as Vx, Vy and Vz.

EXPERIMENTAL SETUP AND METHODOLOGY

Schematic of single cylinder optical research engine equipped with PIV system is shown in figure 1.

Experiments were conducted on a single cylinder optical research engine (AVL 5402) coupled with an AC dynamometer. Test engine is equipped with fuel conditioning, lubricating oil conditioning and coolant condition systems for conducting investigations at various engine operating conditions. For the current investigations, lubricating oil temperature and coolant temperature were kept constant (80°C and 60°C respectively) for the entire duration of experiments. Engine load and speed were controlled by AC dynamometer (Wittur Electric Drives, 2SB 3). This dynamometer can motor the engine upto 3000 rpm. State-of-the-art intake air measurement system (ABB Automation, Sensy-flow P), gravimetric fuel flow meter (AVL, 733S.18) were used for performing engine tests. In-cylinder pressure was measured using a piezoelectric pressure transducer (AVL, QC34C) and charge amplifier along with a high speed combustion data acquisition and analysis system (AVL, Indismart) on a crank angle basis using a high precision shaft encoder (AVL,365CC/ 365X). Maximum motoring pressure for optical head assembly is 34 bar. Technical specifications of the test engine are given in table 1.

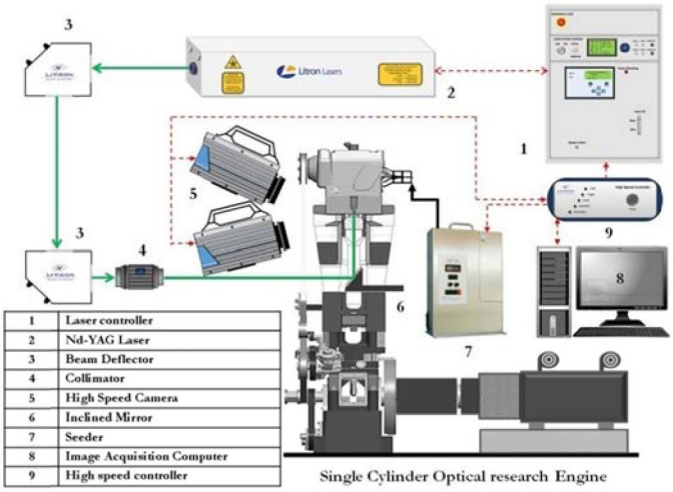

Figure 1. Schematic of SCORE with PIV

Table 1. Technical specifications of SCORE

Engine Type	AVL 5402
Number of cylinders	1
Bore/ stroke	85/ 90 mm
Swept volume	510.7 cc
Compression Ratio	17.5
Inlet port type	Tangential and Swirl Inlet Port
Maximum power	6 kW
Maximum Engine speed	2500 rpm
Fuel Injection Pressure	200-1400 bar
Fuel system	Common Rail Direct Injection
High Pressure System	Common Rail CP4.1 BOSCH
Engine Management System	AVL-RPEMS+ ETK7 (Bosch)
Valves per cylinder	4 (2 inlet, 2 exhaust)
Valve train type	DOHC cam follower
Liner type / base	Wet

For PIV experiments, optical head assembly of test engine was used. In this system, engine has a full length quartz liner and a sapphire window in the piston crown to provide full optical access of the combustion chamber. A high pressure air jet was supplied below extended piston for piston cooling. Constant 60°C coolant temperature was used to avoid thermal concentration in quartz window. PIV setup consisted of a double pulse Nd:YLF laser (Litron, LDY series Laser) with maximum output 150W was used as the light source for illumination for seeding particles. Two beam deflectors were used to direct the laser beam in the desired direction to a collimator. The collimator converts the laser beam into a light sheet which was deflected by a 45° inclined mirror which is fixed inside the extended piston. This piston has a sapphire window in the piston crown from where laser sheet enters inside the optical combustion chamber of engine. The quartz optical window provided optical

access to the combustion chamber. The laser sheet was aligned with the central axis of the cylinder in line with the fuel injector. Two high speed CCD cameras (LaVision, 1024×1024 pixels, 12 bits) having schiempflug adapters were used in double frame mode (Frame rate 2500 Hz) to capture the images. For the visualization of flow pattern, intake air was seeded with graphite particles at 2.5 bar pressure using solid particle disperser (Palas, RBG 1000). For the experiments, calibration was performed in the centre plane along the central axis of combustion chamber where the laser sheet was aligned just beneath the injector. A rectangular two level 3-D calibration plate and polynomial calibration model was used to perform the calibration.

Davis 8.2 software (LaVision) was used to perform the Tomographic processing of the images. As a part of pre-processing of the images, 5×5 sliding minimum was subtracted from the images to get a constant background across the images. For smoothening of vector field, Gaussian smoothing of 3×3 pixels was applied during analysis. Geometric mask was used to select the desired area in the captured images. The volume reconstruction of the images was done using Fast MART (Multiplicative Algebraic Reconstruction Technique). Direct correlation was done for volume correlation with four window sizes, first being 128 voxel with 75% overlap and other 3 being 64 voxels with 75% overlap with decreasing volume binning for each step. This was followed by vector post-processing in which universal outlier detection was done to remove spurious vectors. A Gaussian smoothing of 3×3×3 and a second order polynomial filter was applied during post processing to the vector fields. Practical experimental setup used for PIV experiments is shown in figure 2.

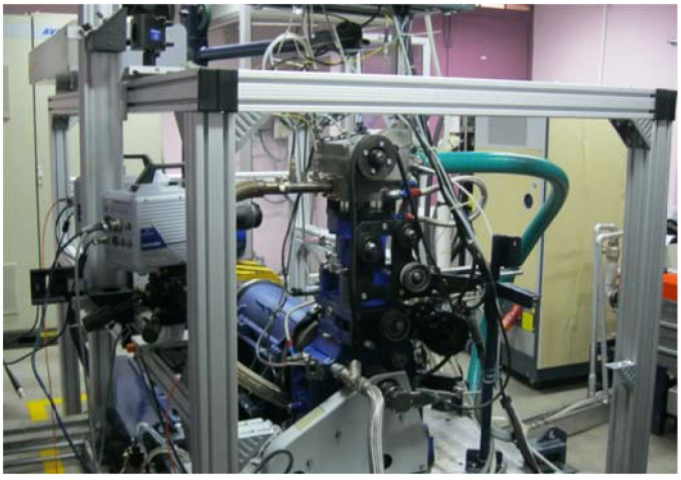

Figure 2. Practical setup of SCORE with PIV

RESULT AND DISCUSSIONS

In this research, Tomographic PIV was performed for Z = 9 mm and results are represented for Z = 1 mm, 3 mm, 5 mm, 7 mm and 9 mm (5 different z positions). Z= 5 mm being the centre planealong the central axis beneath the fuel injector.Z= 1 mm and Z= 3 mm being near the intake valve and Z= 7 mm and Z= 9 mm being near the exhaust valve. To investigate the air flow characteristics, engine was motored at two different engine speeds as 1200 and 2100 rpm. For analysis, two different piston positions as 270° bTDC and 90° bTDC were selected during intake and compression stroke respectively. For the experiments a volume of 48×28×9 mm^3 was chosen for image analysis as shown in figure 3.

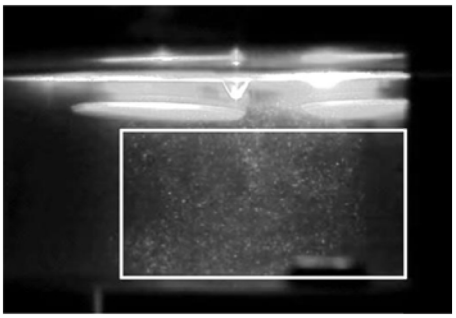

Figure 3. Area of interest for image analysis

For PIV experiments, calibration was performed through the optical window in order to take into account the optical distorions due to window curvature during the PIV imaging. Piston crown window diameter was 48mm, compared to 85mm bore diameter and the light sheet passing thriugh the window was not sufficient to illuminate entire width of the combustion chamber. Enlargement of the piston crown window is required for the investigation of flows near the combustion chamber wall. Image noise due to flares caused by film fogging also prevented measurements close to the combustion chamber walls. Appropriate camera focusing and optical corrections help reduce laser pulse energy, which illuminates the seed particles. For pulse energies below 75 mJ, scattered light level in the camera image plane was found to vary directly proportional to the illuminating laser pulse energy however for higher laser pulse energies, flare increased at a greater rate.

Velocity Analysis

Velocity profiles at two engine speeds as 1200 and 2100 rpm were analysed at different Z locations and compared. Significant changes in flow pattern was observed in velocity profile along with variations in velocity for both engine speeds. For better understanding of the the velocity profile, streamlines were also drawn during image analysis. During the intake stroke (270° bTDC), velocity profile is shown in figure 4 for 1200 and 2100 rpm at Z= 3mm and 7mm. Tumble motion can be seen in Figure 4(a) due to circulation of air due to reverse motion of air from the piston after it strikes the piston. In figure 4(b), a stagnation point is observed at x= 23mm, y= −1mm. At this point air from the inlet valves and piston meet and a point of convergence arises. At 1200 rpm, the velocity range in the considered area of interest ranges from 0-14.5 m/s. Similarly, at 2100 rpm, stagnation points were observed in both cases (Z locations). Tumble motion is also observed in case of 2100 rpm which is relativily stronger near the piston. Sudden change in the direction of air motion is the main reason for this finding. The velocity range at 2100 rpm is found 0-19 m/s which is comparitively higher compared to 1200 rpm due to higher engine speed.

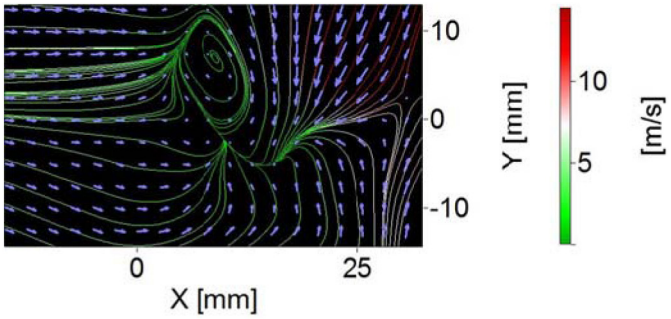

a. Velocity at 270°bTDC, Z= 3 mm and at 1200 rpm

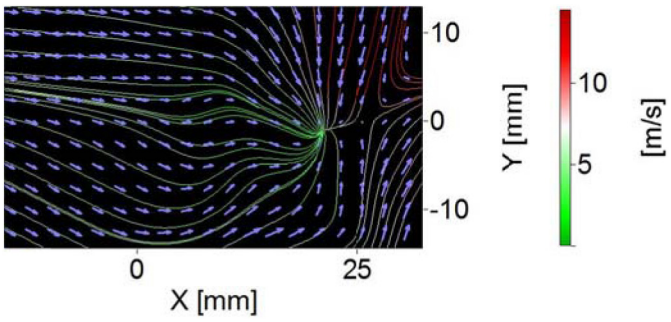

b. Velocity at 270° bTDC, Z= 7 mm and at 1200 rpm

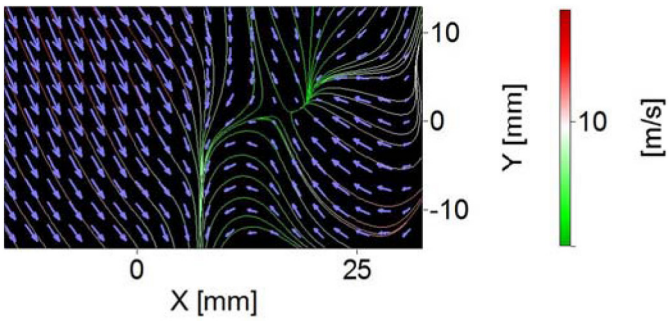

c. Velocity at 270° bTDC, Z= 3 mm and at 2100 rpm

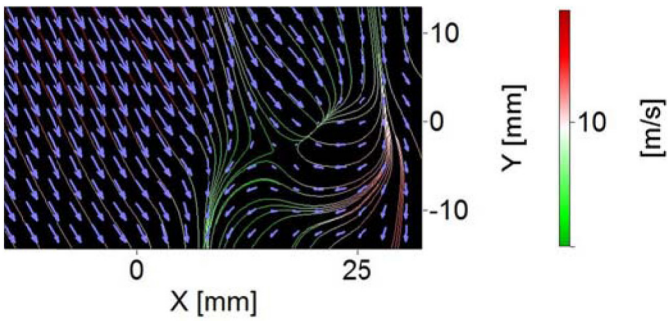

d. Velocity at 270° bTDC, Z= 7 mm and at 2100 rpm

Figure 4. Velocity analysis at different Z planes and engine speeds in intake stroke

From figure 4(a) and 4(b) shows higher air velocity beneath intake valve as compared to near exhaust valve. This higher velocity resulted more turbulence which improvers air flow pattern inside the combustion chamber. Similarly at 2100 rpm engine speed (figure 4(c) and 4(d)), stagnation point for Z= 3mm is slighlty higher as compared to Z= 7 mm. It reflects higher air velocity near intake valve (Z= 3 mm) which shifts stagnation point slighlty above compared to exhaust valve (Z= 7mm). At higher engine speeds, air velocity pattern follows piston movement path (vertical) in a better manner compared to low engine speeds. At 2100 rpm, air velocity pattern is vertical however at 1200 rpm, it follows horizontal pattern. At 2100 rpm, stagnation zone is wider as compared to 1200 rpm and it was found increasing with movement away from intake valve.

During compression stroke, different air flow pattern was found due to upward movement the piston that forces air to move away from piston. The velocity also considerably reduced in the compression stroke due to absence of the high velocity intake air from intake valves.Results are displayed at piston position 90° bTDC at Z= 1, Z= 5 mm and Z= 9 mm at two different engine speeds as 1200 rpmand 2100 rpm. During comression stroke, cyclic air motion was observed at both engine speeds. Air flow patterns were also varried at different z locations. Near TDC, significantly higher vortex formation can be observed at 2100 rpm compared to 1200 rpmwhich represents strong tumble motion of air. Similar to intake stroke, air velocity is significantly higher at 2100 rpm compared to 1200 rpm. At 1200 rpm, air velocity varried from 0-9.4 m/s while at 2100 rpm, it is found 0-17 m/s. In compression stroke, effect of Z position can be clearly observed. Maximum air velocity was found near intake valve (Z= 1mm) however it decreased with increasing distance from intake valve (Z= 5mm amd Z= 9mm). Figure 5(a) also shows maximum turbolence near intake valve which get reduced in figure 5(b) and 5(c).

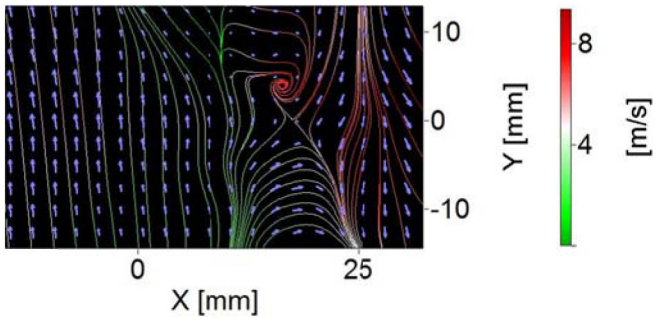

a. Velocity at 90° bTDC, Z= 1 mm and at 1200 rpm

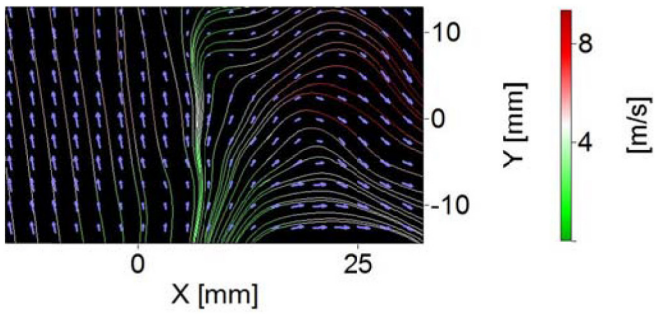

b. Velocity at90° bTDC, Z= 5 mm and at 1200 rpm

Figure 5. Velocity analysis at different Z planes and engine speeds in compression stroke

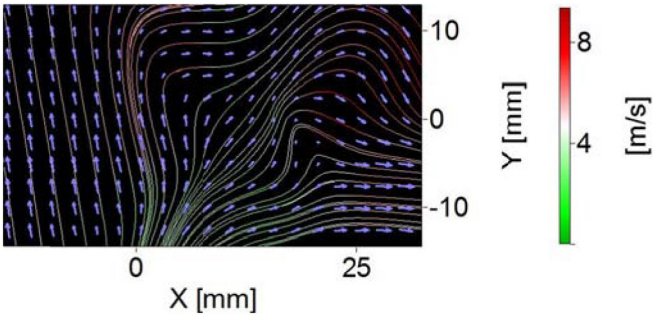

c. Velocity at90° bTDC, Z= 9 mm and at 1200 rpm

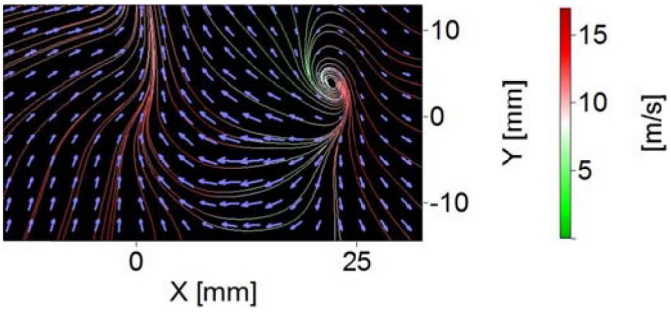

d. Velocity at90° bTDC, Z= 1 mm and at 2100 rpm

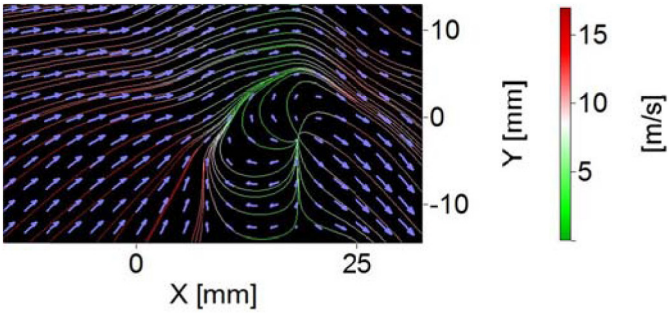

e. Velocity at 90° bTDC, Z= 5 mm and at 2100 rpm

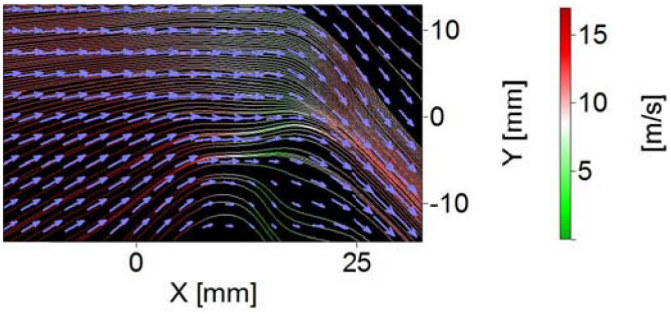

f. Velocity at 90° bTDC at Z= 9 mm and 2100 rpm

Figure 5. (cont.) Velocity analysis at different Z planes and engine speeds in compression stroke

Comparison of figure 5(a, b, c) and figure 5(d, e, f) shows that Z position affercs air flow pattern at higher engine speed (2100 rpm) compared to lower engine speed (1200 rpm). At 2100 rpm, stagnation point for Z= 5mm, clearly indicats the reversal effect of air coming from piston. As Z position moves away from intake valve, less turbulence due to relativily lower air velocity can be observed.

Vorticity Analysis

Voriticity can be defined as rotation of a flow field at microscopic level. Vorticity is of critical importance especially in IC engines as it aids in studying and analyzing turbulent characteristics of air flow inside the combustion chamber. It affects the air-fuel mixing as well as heat transfer that directly controls engine combustion and performance. Vorticity analysis was performed using velocity vectors at 1200 rpm and 2100 rpm at different Z locations. Figure 6(a) and 6(b) shows the vorticity for 1200 rpm (270° bTDC) at Z= 3 mm and Z= 7 mm followed by Figure 6(c) and 6(d) which show the vorticity for 2100 rpm (270° bTDC) at Z= 3 mm and Z= 7 mm. During intake stroke, maximum vorticity was observed near intake valve and it gets reduced with increasing distance from intake valve. Higher vorticity near intake valves is due to the high velocity intake air coming from the inlet valves and its reversal from the piston after hitting it. Higher vorticity at higher engine speeds is another important finding that was resulted due to high velocity of intake air entering the cylinder. At 1200 rpm, vorticity ranges from 0-2100 1/s while at 2100 rpm, it ranges from 0-2400 1/s.

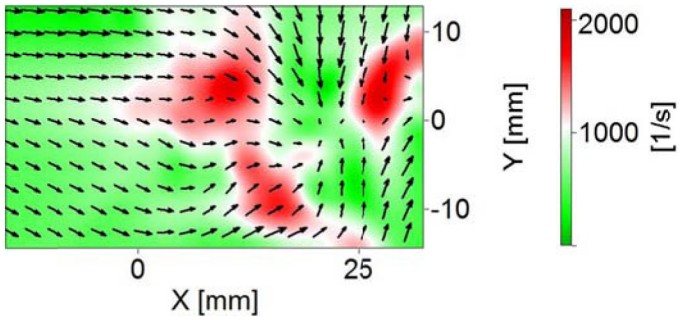

a. Vorticity at 270° bTDC, Z= 3 mm and at 1200 rpm

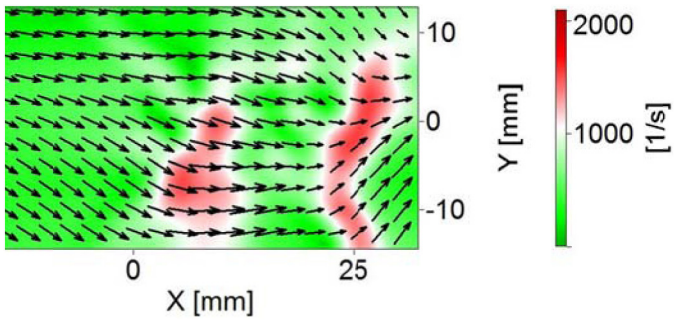

b. Vorticity at 270° bTDC, Z= 7 mm and at 1200 rpm

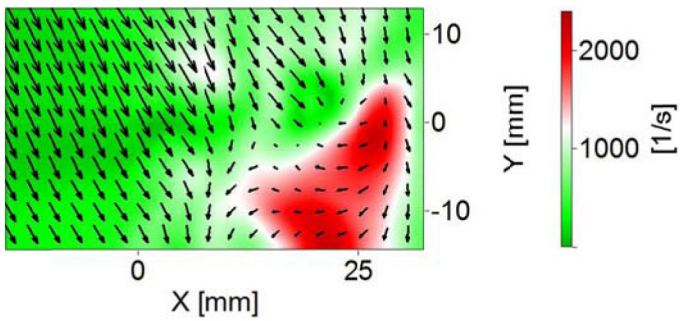

c. Vorticity at 270° bTDC, Z= 3 mm and at 2100 rpm

Figure 6. Vorticity analysis at different Z planes and engine speeds in intake stroke

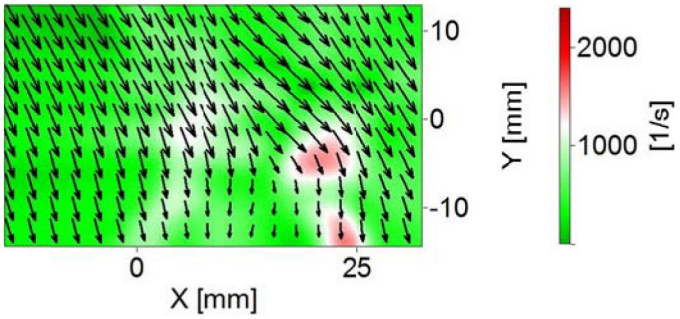

d. Vorticity at 270° bTDC, Z= 7 mm and at 2100 rpm

Figure 6. (cont.) Vorticity analysis at different Z planes and engine speeds in intake stroke

During compression stroke, maximum vorticity reduces to 1700 1/s at 1200 rpm, whereas at 2100 rpm, the maximum vorticity is found to be 2250 1/s. However, small variation in vorticity is also observed at different Z planes. In case of 2100 rpm, vorticity is higher compared to 1200 rpm which is clearly evident due to the fact that the piston is pushing the air above more strongly at higher engine speed leading to a strong rotation of the complete vector field. High vorticity regions were found to be spread more widely at 2100 rpm. This indicates that air flow is more turbulent at 2100 rpm compared to 1200 rpm during the compression stroke. This can be also verified from figure 4(c) and 4(d) where it is clear that the rotation in velocity field is stronger in case of 2100 rpm as compared to 1200 rpm.

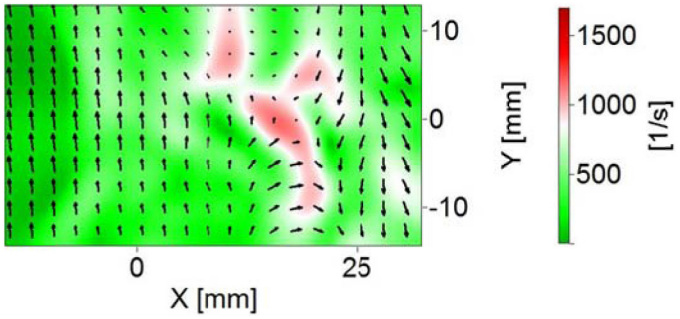

a. Vorticity at 90° bTDC, Z= 1 mm and at 1200 rpm

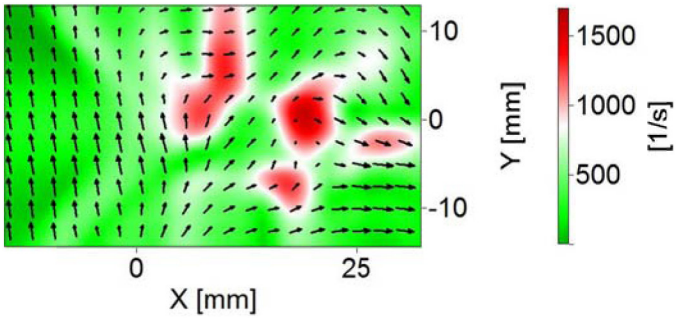

c. Vorticity at 90° bTDC, Z= 9 mm and at 1200 rpm

Figure 7.

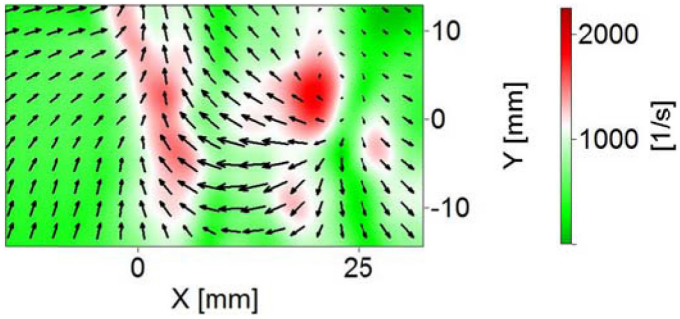

d. Vorticity at 90° bTDC, Z= 1 mm and at 2100 rpm

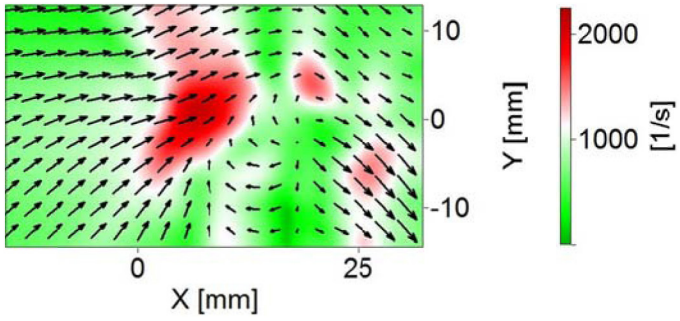

d. Vorticity at 90° bTDC, Z= 5 mm and at 2100 rpm

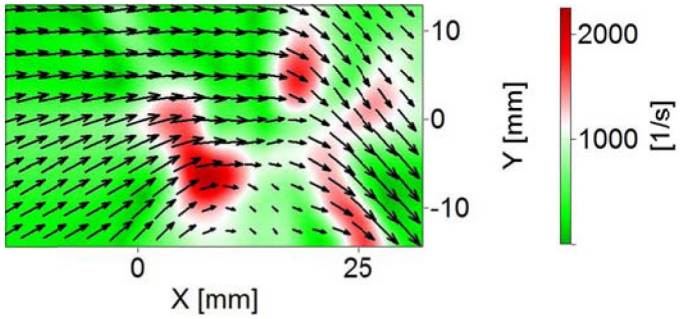

d. Vorticity at 90° bTDC, Z= 9 mm and at 2100 rpm

Figure 7. (cont.) Vorticity analysis at different Z planes and engine speeds in compression stroke

Vorticity analysis at different Z planes provides information about turbulent characteristics of the air flow throughout the volume which cannot be performed using in 2-D PIV. Figure 7(a), 7(b) and 7(c) show vorticity for 1200 rpm (90° bTDC) at Z= 1 mm, Z= 5 mm and Z= 9 mm while figure 7(d), 7(e) and 7(f) show vorticity for 2100 rpm (90° bTDC) at Z= 1 mm, Z= 5 mm and Z= 9 mm. Vorticity was found more distributed near intake valve (Z= 1mm) as compared to exhaust valve (Z= 9 mm) and its magnitude also increases with increasing distance from intake valve. At higher engine speeds, vorticity distribution is slightly different compared to lower engine speeds. At 2100 rpm, vorticity distribution is wider compared to 1200 rpm and its magnitude is also higher which can be also observed in velocity profile (figure 4).

Comparison of Velocity Components (Vx, Vy and Vz)

To get a better understanding of the velocity profile in the considered volume, the components of velocity in X, Y and Z direction at 2100 rpm and at different Z locations have been studied. This gives us a

good idea about the volumetric velocity profile during the intake and compression stroke. Movement from intake side to exhaust side shows the change in velocity pattern for Vx. Near intake valve Vx varies from −5-5 m/s however near exhaust valve it ranges from −28.5 m/s. Reduction in Vy with movement away from intake valve is important observation that occurs due to expansion of air jet from intake valve. Vy become more uniform near exhaust valve compared to intake valve. There is a small change which is observed in the magnitude of Vz. Large variation in Vz as compared to Vx and Vy is another observation of this analysis. During intake stroke all velocity components as Vx, Vy and Vz are found to be increasing with movement along Z direction and range of velocity is higher due to higher engine speed. Maximum velocity range in considered volume for Vx is −11-11 m/s, Vy is −12-12 m/s and Vz is −14.4-14.4 m/s.

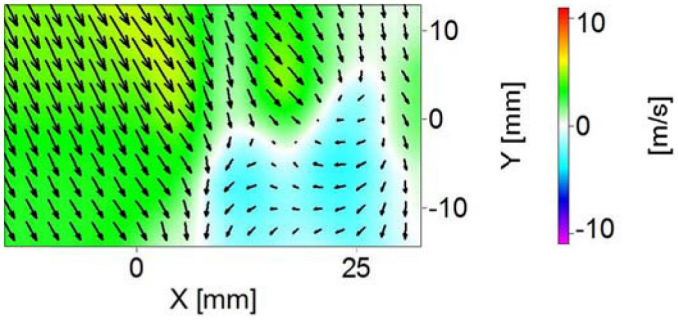

a. Vx at 270° bTDC, Z= 3 mm and at 2100 rpm

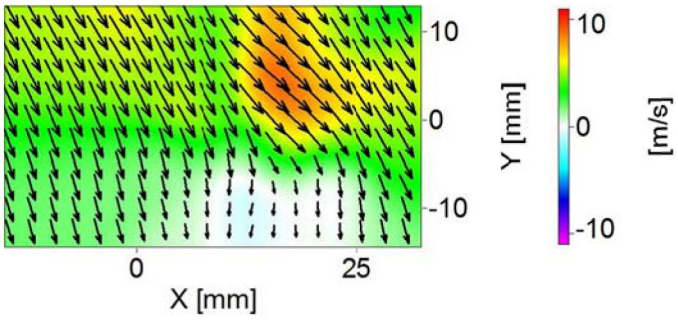

b. Vx at 270° bTDC, Z= 7 mm and at 2100 rpm

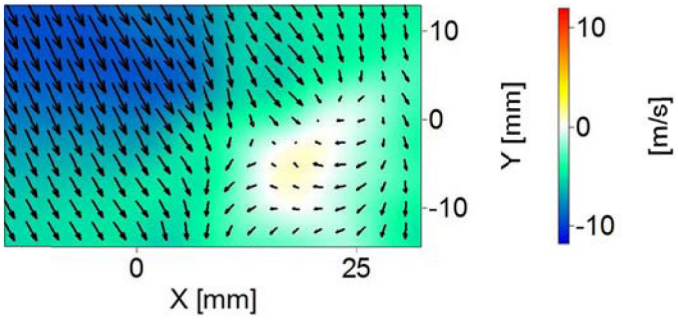

c. Vy at 270° bTDC, Z= 3 mm and at 2100 rpm

Figure 8.

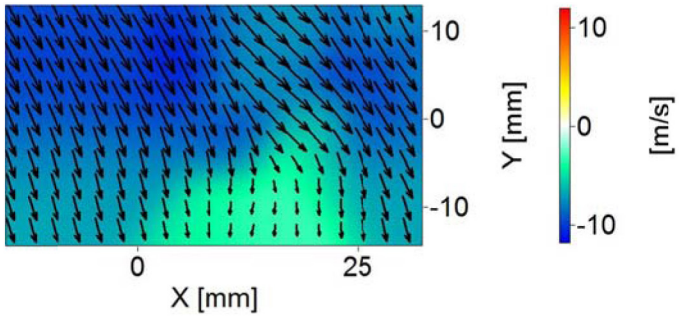

d. Vy at 270° bTDC, Z= 7 mm and at 2100 rpm

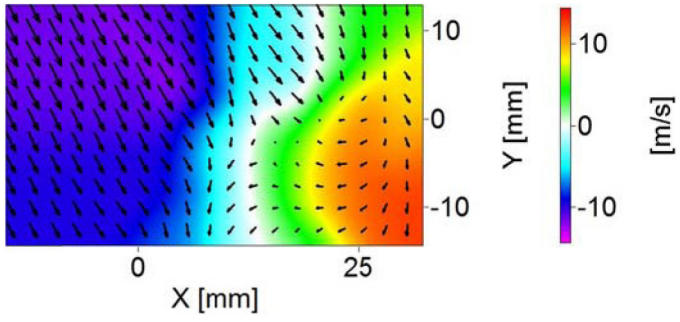

e. Vz at 270° bTDC, Z= 3 mm and at 2100 rpm

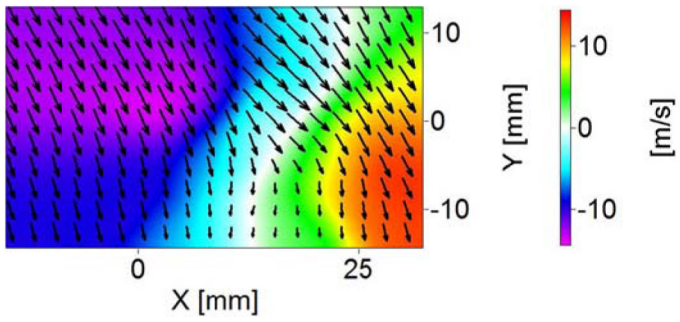

f. Vz at 270° bTDC, Z= 7 mm and at 2100 rpm

Figure 8. (cont.) Vx, Vy and Vz analysis at different Z planes in intake stroke

During compression stroke, 90°bTDC, tumble motion is clearly visible at 2100 rpm which is resulted due to higher reactive force from piston that pushes cylinder air upward and promotes mixing. Higher Vx and Vy can be observed during movement along Z direction and vector orientation indicates a strong clockwise tumble motion being developed inside the combustion chamber. It can be seen that vectors pointing towards the right have positive X velocity and vice-versa. A significant change in Vx with movement away from intake valve is clearly visible in figure 9 (a, b, c). This shows higher mixing tendency during compression stroke. Cyclic movement of air is slightly higher nearer to exhaust valves that are also validated by vorticity results. Vy shows a different flow pattern compared to Vx. Slight reduction in Vy with distance from intake valve shows the effect of intake stroke however Vy also decreases beneath the intake valve. Variation in Vz along the Z direction can be observed and the zone with negative Z velocity is slightly higher near intake valve. In the considered area, zone with higher Vz reduces with increasing distance from intake valve. This gives an

idea about the velocity profile which is generated volumetrically along the Z plane. At 2100 rpm, the range of Vx is −11-11 m/s, Vy is −8-8 m/s and Vz is −15-15 m/s.

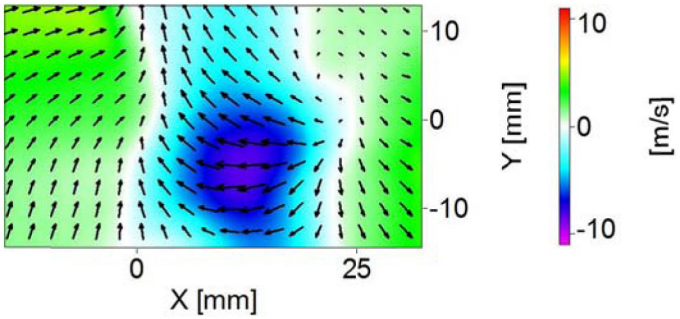

a. Vx at 90° bTDC, Z= 1 mm and at 2100 rpm

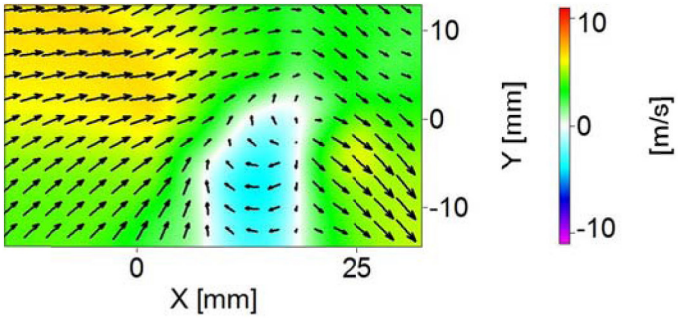

b. Vx at 90° bTDC, Z= 5 mm and at 2100 rpm

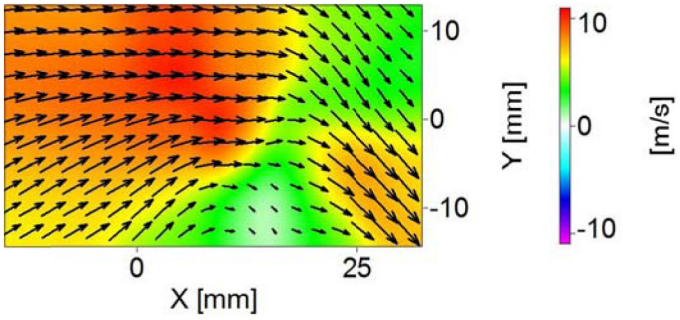

c. Vx at 90° bTDC, Z= 9 mm and at 2100 rpm

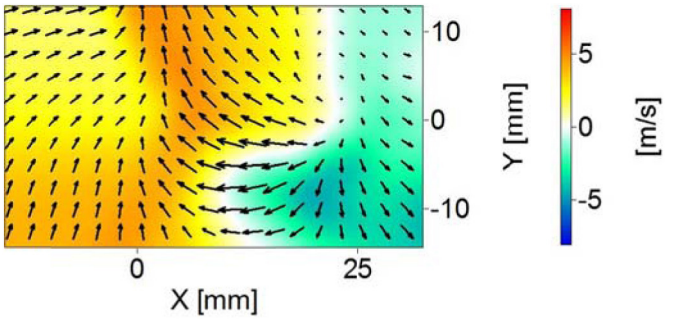

d. Vy at 90° bTDC, Z= 1 mm and at 2100 rpm

Figure 9.

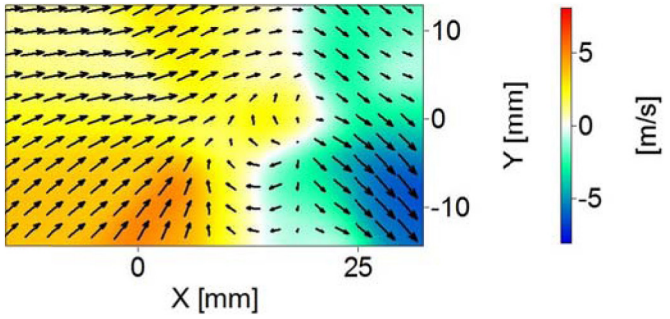

e. Vy at 90° bTDC, Z= 5 mm and at 2100 rpm

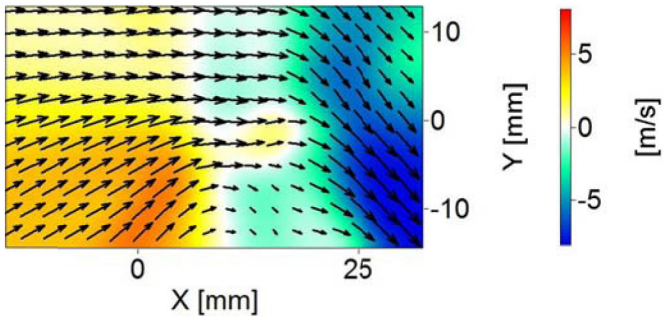

f. Vy at 90° bTDC, Z= 9 mm and at 2100 rpm

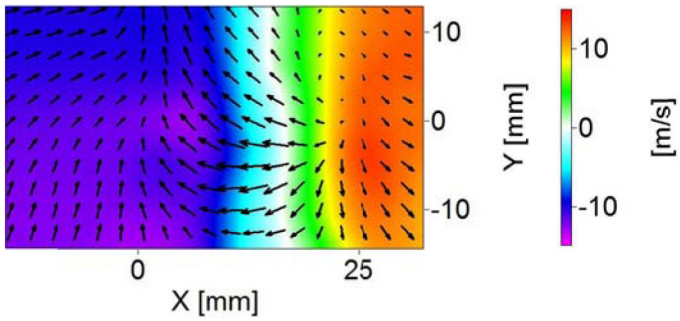

g. Vz at 90° bTDC, Z= 1 mm and at 2100 rpm

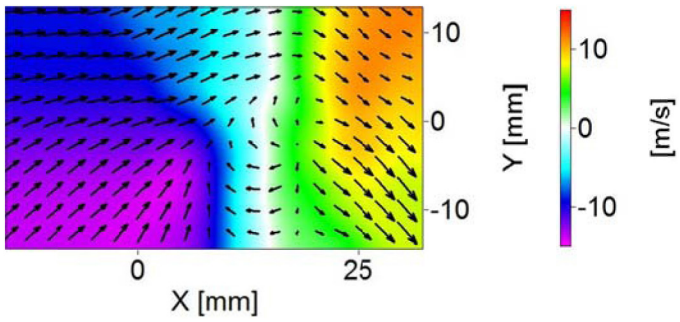

h. Vz at 90° bTDC, Z= 5 mm and at 2100 rpm

Figure 9. (cont.) Vx, Vy and Vz analysis at different Z planes in compression stroke

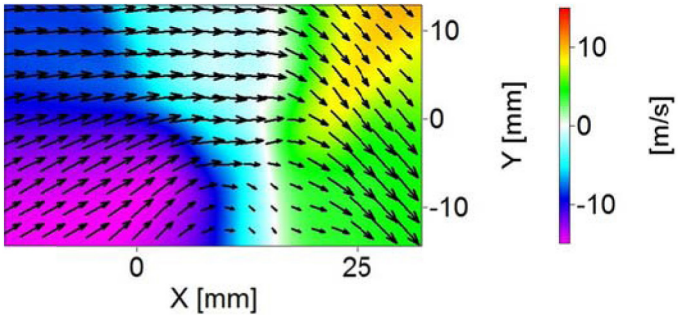

i. Vz at 90° bTDC, Z= 9 mm and at 2100 rpm

Figure 9. (cont.) Vx, Vy and Vz analysis at different Z planes in compression stroke

CONCLUSIONS

In this study, TomographicPIV experiments were performed at two engine speeds (1200 rpm and 2100 rpm) and at different Z locations (Z= 1 mm, 3 mm, 5 mm, 7 mm and 9 mm) to investigate the air flow characteristics inside the combustion chamber. Two different piston positions as 270°bTDC (intake stroke) and 90°bTDC (compression stroke) were selected for the analysis of various flow parameters. To characterize the air motion, velocity, vorticity and different components of velocity as Vx, Vy and Vz were investigated. In the experiments, air velocity was found to be significantly affected by engine speed and it is higher for higher engine speed. Air velocity was also affected distance from intake stroke. During intake stroke, air velocity is higher beneath of intake valve and decreased with distance from intake valve. During compression stroke, air velocity is slightly lower due to upward movement of piston. Higher turbulence during compression stroke is another important observation. Vorticity analysis shows higher vorticity at higher engine speed. During compression stroke, vorticity magnitude and regions of maximum vorticity is wider compared to intake stroke. This behavior is important for CI engines because it promotes better fuel-air mixing and affects engine performance and emission characteristics. Different velocity components as Vx, Vy and Vz show relative dominance at different operating conditions. Highly distributed regions of these components are beneficial which enhance fuel-air mixing. Effect of different Z locations on Vz and maximum variation in Vz is very important finding of this study. This shows that fuel-air mixing is significantly affected by Vz and it cannot be measured by 2D PIV. Finally it can be concluded that time-resolved high-speed Tomographic PIV provides important information of in-cylinder flow characteristics due to its measurement capability of all three components of velocity within a volume.

REFERENCES

1. Dierksheide, U., Meyer, P., Hovestadt, T. and Hentschel, W., "Endoscopic 2D Particle Image Velocimetry (PIV) Flow Field Measurements in IC Engines," Experiments in Fluids 33:794800, 2002.
2. Block, B., Hentschel, W. and Oppermann, W., "PIV in-cylinder Tumble Flow Measurements in an IC-Engine. In: Adrian R, Hassan Y, Meinhart C (eds) Proc. 3rd Int. Workshop on Particle Image Velocimetry, Santa Barbara, Calif. 631-636, 1999.
3. Xiong, W. and Merzkirch, W, "PIV Experiments using an Endoscope for Studying Pipe Flow," J Flow Visualization Image Process 6:167-175, 1999.
4. Pickering, C. J. D. and Halliwell, N. A., "Particle Image Velocimetry: A New Field Measurement Technique," In Optical Measurement in Fluid Dynamics, Inst. Phys. Conf., Series no. 77, session 4. Adam Hilger, Bristol, 1985.
5. Adrian, R. J., "Particle-Imaging Techniques for Experimental Fluid Mechanics," Annu. Rev. Fluid Mech., 23: 261-304, 1991.
6. Coupland, J. M. and Halllwell, N. A., Particle Image Velocimetry: Rapid Transparency Analysis using Optical Correlation. Appl. Optics, 27: 919-1921, 1988.
7. Huntley, J. M., An image processing system for the Analysis of Speckle Photographs. J. Phys. E (Sci. Znstr.), 13: 579-584, 1980.
8. Druault, P., Guibert, P. and Alizon, F., "Use of Proper Orthogonal Decomposition for Time Interpolation from PIV Data," Exp. Fluids 39: 1009-1023, 2005.
9. Funk, C., Sick, V., Reuss, D., and Dahm, W., "Turbulence Properties of High and Low Swirl In-Cylinder Flows," SAE Technical Paper 2002-01-2841, 2002, doi:10.4271/2002-01-2841.
10. Reuss, D., "Cyclic Variability of Large-Scale Turbulent Structures in Directed and Undirected IC Engine Flows," SAE Technical Paper 2000-01-0246, 2000, doi:10.4271/2000-01-0246.
11. Fajardo, C. M. and Sick, V., "Flow Field Assessment in a Fired Spray-Guided Spark-Ignition Direct-Injection Engine Based on UV Particle Image Velocimetry with Sub Crank Angle Resolution," Proc. Combust. Inst. 31: 3023-3031, 2007.
12. Voisine, M., Thomas, L., Boree J. and Rey, P., "Spatio-temporal Structure and Cycle to Cycle Variations of an in-cylinder Tumbling flow," Exp. Fluids 50:1393-1407, 2011.
13. Müller, S.H.R., Böhm, B., Gleißner, M. Grzeszik, R. et al., "Flow Field Measurements in an Optically Accessible, Direct-Injection Spray-Guided Internal Combustion Engine using High-Speed PIV," Exp. Fluids 48: 281-290, 2010.
14. Coupland, J. M. and Pickering, C. J. D., "Particle Image Velocimetry: Estimation of Measurement Confidence at Low Seeding Densities," Optics Lasers Engng, 9: 201-210, 1988.
15. Keane, R. D. and Adrian, R. J., "Optimisation of Particle Image Velocimeters. Part 1: Double Pulsed Systems. Meas. Sci. Technol., 1:1202-1215, 1990.
16. Grant, I. and Owens, E. H., "Confidence Interval Estimates in PIV Measurements of Turbulent Flows. Appl. Optics, 29:1400-1402, 1990.
17. Hinsch, K., Arnold, W. and Platen, W., Turbulence Measurements by Particle Imaging Velocimetry. L.I.A. 60 ICALEO, 127-134, 1987.
18. Adrian, R. J., "Double Exposure, Multiple-field Particle Image Velocimetry for Turbulent Probability Density. Optics Lasers Engng, 9: 211-228, 1988.
19. Prasad, A. K., Adrian, R. J., Landreth, C. C. and Offutt, P. W., "Effect of Resolution on the Speed and Accuracy of Particle Image Velocimetry Interrogation. Exp. Fluids, 13:105-116, 1992.
20. Reeves, M., Towers, D.P., Tavender, B. and Buckberry, C.H., "A High-Speed All-Digital Technique for Cycle-Resolved 2-D Flow Measurement and Flow Visualization within SI Engine Cylinders. Optics and Lasers in Engineering, 31:247-261, 1999.
21. Stansfield, P., Wigley, G., Justham, T. and Catto, J. et al., "PIV Analysis of In-cylinder Flow Structures over a Range of Realistic Engine Speeds," Experiments in Fluids, 43 (1):135-146, 2007.
22. Calendini, P., Duverger, T., Lecerf, A., and Trinite, M., "In-Cylinder Velocity Measurements with Stereoscopic Particle Image Velocimetry in a SI engine," SAE Technical Paper 2000-01-1798, 2000, doi:10.4271/2000-01-1798.
23. Dannemann, J., Pielhop, K., Klaas, M. and Schroder. W., "Cycle Resolved Multi-Planar Flow Measurements in a Four-Valve Combustion Engine," Exp Fluids, 50:961976, 2010.
24. Maas, H.G., Gruen, A. and PapantoniouD., "Particle Tracking Velocimetry in Three-Dimensional Flows," Exp. Fluids 15:133-146, 1993.
25. Brucker C.H., "3D Scanning PIN Applied to an Air Flow in a Motored Engine using Digital High Speed Video," Meas. Sci. Technol. 8:1480-1492, 1997.
26. Konrath, R., Schroder, W. and Limberg, W., "Holographic Particle Image Velocimetry Applied to the Flow within the Cylinder of a Four-Valve Internal Combustion Engine," Exp. Fluids 33:781-793, 2002.
27. Kitzhofer, J., Brucker, C. and Nonn, T., "Generation and visualization of volumetric PIV data fields," Exp Fluids 51: 1471-1492, 2011.
28. Elsinga, G.E., Scarano, F., Wieneke, B. and Oudheusden B.W.V., "Tomographic particle image velocimetry," Exp. Fluids 41:933-947, 2006.

29. Baum, E., Petersona, B., Surmann, C., Michaelis, D. et al., "Investigation of the 3D Flow Field in an IC Engine using Tomographic PIV," Proceedings of the Combustion Institute, doi.org/10.1016/j.proci.2012.06.123.

CONTACT INFORMATION

Dr Avinash K Agarwal, FSAE, FASME
Poonam and Prabhu Goyal Endowed Chair Professor
Department of Mechanical Engineering
Indian Institute of Technology Kanpur
Kanpur-208016 India
www.iitk.ac.in/erl
Tel: +91 512 2597982 (Off)
Fax: +91 512 2597982, 2597408 (Off)
akag@iitk.ac.in

ACKNOWLEDGMENTS

Financial support from Council for Scientific and Industrial Research (CSIR), Government of India's SRA scheme to Akhilendra Pratap Singh is acknowledged, which supported his stay at IIT Kanpur for conducting these experiments.

DEFINITIONS/ABBREVIATIONS

PIV - Particle Imaging Velocimetry

SI - Spark Ignition

SCORE - Single Cylinder Optical Research Engine

CCD - Charge Coupled Device

MART - Multiplicative Algebraic Reconstruction Technique

bTDC - Before Top Dead Center

Vx - Velocity in X direction

Vy - Velocity in Y direction

Vz - Velocity in Z direction

TPIV - Tomographic Particle Image Velocimetry

DISI - Direct Injection Spark Ignition